VOLUME 31, 2, 258–268
TRIBOLOGY TRANSACTIONS

Frictional Instabilities in Ball Bearings©

PRADEEP K. GUPTA (Member, STLE)
PKG Inc.
Clifton Park, New York 12065

Computer modeling techniques are used to investigate instabilities in the motions of ball and cage in a ball bearing. As the friction at ball/race and ball/cage contacts increases, the cage mass center whirl orbit changes from circular to polygonal and then to a rather erratic shape under excessive friction. The corresponding variations in whirl velocities also increase to represent bearing squeal. It is shown that cage instabilities are directly dependent on the ball/race traction slope, under low slip velocities, and the friction coefficient at the cage interfaces. Under steep traction slopes, the variation in traction at higher slip rates is also significant in high-speed bearings. In particular, it is found that a negative traction slope, in the high-slip region, may produce appreciable ball skid which promotes excessive interaction in the cage pockets and, perhaps, the most damaging instability of the cage, where the mechanical interactions progressively increase to indicate significant potentials for cage failure. Under stable conditions of operation, the computer results also provide correlations between time-averaged wear rates of the cage and the frictional behavior.

INTRODUCTION

It is well established that lubrication plays a dominant role in determining the performance and overall life of a rolling bearing. The friction or traction forces between the interacting bearing elements (rolling elements, cage and the races) not only determine the nominal wear life of the bearing but they are often responsible for exciting certain instabilities in the motion of the bearing elements. The instabilities, in turn, lead to premature and rather catastrophic bearing failures. The understanding of such an intricate dynamic coupling between the frictional behavior of the lubricant and the performance of the bearing is, therefore, crucial to bearing design for advanced applications. Furthermore, with the increasing demand of higher operating temperatures and speeds, it has become essential to replace the conventional oils and greases by solid lubricants, the behavior of which adds an additional degree of complexity. Also, since the traction coefficients are relatively higher with the solid lubricants, the problem of correlating the dynamic performance of a bearing to the traction coefficients between interacting bearing elements becomes increasingly important. As a first step to the development of such a correlation, a parametric evaluation of the dynamic performance of a high-speed ball bearing as a function of the traction behavior at the ball/race, ball/cage and cage/race interactions is the primary objective of the present investigation.

Analytical modeling and computer simulation of bearing performance have proven to be very effective in characterizing bearing behavior over a large range of parameters. The recent advancements in computing techniques and analytical simulation of complex mechanical systems have resulted in significant developments in the modeling of the dynamic performance of a rolling bearing. The conventional quasi-static equilibrium models have been replaced by fully dynamic models which integrate the equations of motion of each bearing element and provide a real-time simulation of bearing performance (*1*)–(*12*). The available computer codes offer varying levels of sophistication in modeling the performance of rolling bearings. As an advancement to the earlier codes DREB (*3*), (*5*), (*6*) and RAPIDREB (*8*), (*10*), the recent computer code, ADORE (Advanced Dynamics of Rolling Elements), offers extensive capability for the modeling of frictional behavior, wear and geometrical irregularities in various types of rolling bearings (*11*). Although a few attempts to study the frictional behavior in ball bearings have been made in the past (*4*), (*13*), (*14*), the simulation of bearing instabilities has only been possible under greatly simplified conditions and such investigations have only proven the need for further development in order to understand the complex bearing behavior.

The present investigation employs the computer code ADORE to model the performance of a high-speed ball bearing as a function of the traction behavior of the lubri-

Presented at the 42nd Annual Meeting in Anaheim, California May 11–14, 1987 Final manuscript approved October 29, 1986

cant. A baseline bearing design for a typical high-speed turbine is established and the general motion of the bearing elements is simulated as a function of the frictional behavior at ball/race, ball/cage and cage/race interactions.

MODELING APPROACH

The general behavior of traction, for most liquid and some solid lubricants, as a function of slip velocity in a rolling/sliding contact is shown in Fig. 1; the variation may be written algebraically as:

$$f = [A + Bv] \exp(Cv) + D$$

where f is the traction coefficient, v is the slip velocity and A, B, C, and D are coefficients of the model which are generally determined from experimental investigations.

It has been established that both the slope of the traction curve at very low slip velocities and the variation of traction coefficient at high slip rates have a significant effect on the motion of bearing elements (*15*). By a selective variation of the coefficients, the performance of the bearing is, therefore, modeled over a number of traction curves and overall stability of the bearing elements is established.

With particular emphasis on solid lubricants, the traction behavior at the ball/race contact is also modeled by a more simplified form, shown in Fig. 2. Such a variation has been experimentally proven (*16*), (*22*) to be valid for a number of solid lubricants. Algebraically, the variation in traction may be written as:

$$f = Bv \quad v \leq V$$

$$f = D \quad v > V$$

Unlike the ball/race contacts, interactions at the ball/cage and cage/race interfaces are of pure sliding nature and the sliding velocities for most applications are quite high. It is, therefore, reasonable to model the frictional behavior at these interactions by a constant coefficient of friction.

For the above models of frictional interactions at ball/race, ball/cage, and cage/race contacts, the classical differential equations of motion of all the balls and cage are solved simultaneously and the stability of the bearing elements is

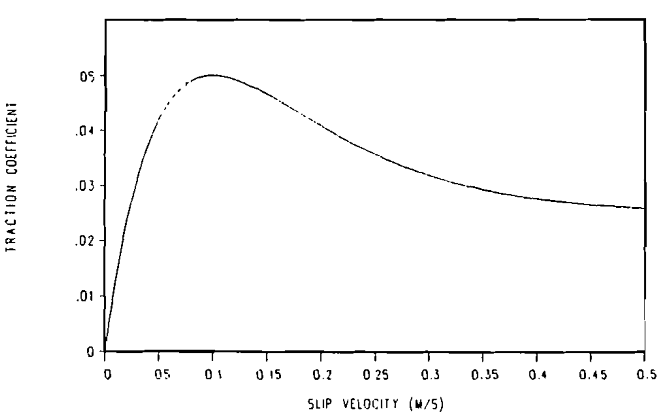

Fig. 1—The general shape of traction-slip curve at the ball/race interface, for most liquid lubricants.

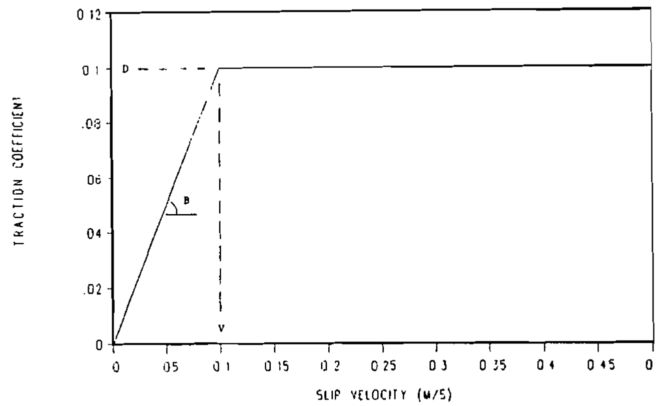

Fig. 2—The general shape of simplified traction-slip relation at the ball/race interface, for most solid lubricants.

investigated as a function the frictional behavior. Details of the interaction models, formulation of the equations of motion, and the computer program, ADORE, used to integrate the equation of motion and model the bearing performance, are well documented elsewhere (*11*).

Stability of the balls is viewed in terms of the variation in sliding velocity, or skid, at the ball/race interface, while cage stability is considered in terms of variations in mass center whirl velocities, nature of the whirl orbit, and overall mechanical interaction at the ball/cage and cage/race contacts. Large variations in mass center whirl velocity have been proven, experimentally, to be representative of bearing squeal and cage instability (*17*). Shape of the whirl orbit is directly dependent on forces exerted on the cage and the resulting variations in the radial and whirl velocities of the cage mass center. For example, a steady cage/race contact force may produce a circular orbit, while the orbit may be somewhat polygonal under periodic cage/race and ball/cage collisions, and the cage mass center may exhibit rather random excursions when the forces exerted have no defined pattern.

Although the instabilities associated with irregular whirl velocities and mass center orbits may produce excessive noise and torque variation in the bearing, they may not result in actual mechanical failure of any of the bearing elements; excessive dynamic collision forces on the cage, on the other hand, may result in physical destruction of the cage and a rather catastrophic bearing failure. Such an instability is indicated by continually increasing level of severity of cage interactions, irrespective of variations in whirl velocity and orbit shape. Since both increasing forces and sliding velocities may result in a mechanical failure of the cage, a positive gradient in a time-averaged wear rate (*18*) of the cage represents a catastrophic situation.

In terms of the classical Archard wear equation, the time-averaged wear rate, W, at any time, T, is to be written as

$$W(T) = \frac{1}{T} \int_{O}^{T} K \frac{P\,V}{H}\, dt$$

where P is the contact load, V is the sliding velocity, K is a wear coefficient, and H is hardness of the cage material.

Although the present investigation considers only the Archard form of wear equation, other more recently developed wear relations (*19*)–(*22*) may be considered in a similar manner. In all cases, a well-defined positive derivative of W with respect to T indicates the highly undesirable form of instability.

BEARING GEOMETRY AND OPERATING CONDITIONS

Since the objectives of the present investigation are to establish trends of bearing performance as a function of traction behavior and demonstrate feasibility of the computer modeling approach for practical bearing designs, a 30-mm angular contact ball bearing is arbitrary selected. The baseline design, outlined in Table 1, is typical of a high-speed turbine engine application. Also, to emphasize a solid-lubricated application, silicon nitride balls, M50 steel races, and a carbon-reinforced composite cage is assumed; the various material properties are also outlined in Table 1. The hardness and wear coefficient values are quite arbitrary; however, since these values are simply used as "scale factors" in the computation of wear rates, they do not effect any of the trends reported herein.

Again, typical of a high-speed turbine engine application, the bearing is assumed to operate at a shaft speed 70,000 rpm with a thrust load of 1000 N and a rotating load of 500 N. The rotating load essentially simulates a shaft unbalance.

The ball/cage and cage/race friction coefficients are considered in the range of 0.010 to 0.20, while the ball/race traction is modeled in terms of the two models discussed above. Figures 3 and 4 show the specific variations investigated. Note that each model is denoted by a curve number; this number is referenced, in the following discussion of the results to denote specific traction variation.

RESULTS

At the operating conditions described above, simulations of bearing performance, over a number of shaft revolutions, as a function of the traction parameters are obtained by running the computer program ADORE. Figure 5* shows the simulated load and contact angle variation at the ball/race contacts, obtained with ball/race traction curve #1 and with a constant coefficient of friction of 0.050 at the cage interactions. Due to a substantial centrifugal force on the ball, at the high operating speed, the contact loads at the outer race are significantly higher. The sinusoidal variation is a result of a combined radial and axial load and the shift of the peaks from once per every rotation of ball center

* All figures are presented as produced by ADORE. Note the remote exponent on the various axes, 10^n is written as 10**n.

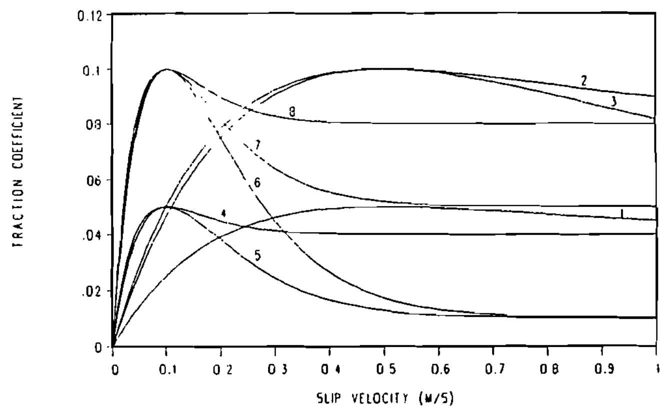

Fig. 3—Ball/race traction curves for a range of traction parameters

Table 1—Bearing Geometry and Material Properties		
Number of Balls	=	17
Ball Diameter	=	6 mm
Pitch Diameter	=	38 mm
Contact Angle	=	20 degrees
Outer Race Curvature Factor	=	0.52
Inner Race Curvature Factor	=	0.54
Bearing Bore	=	30 mm
Bearing Outside Diameter	=	47 mm
Outer Race Fit	=	0
Inner Race Fit	=	20 micron
Cage Outside Diameter	=	41 mm
Cage Inside Diameter	=	37 mm
Cage Width	=	10 mm
Guide Land Clearance (Outer Race)	=	0.25 mm
Pocket Clearance	=	0.25 mm

	Material Properties				
Element	Density Kgm/M**3	Elastic Modulus N/M**2	Poisson's	Hardness N/M**2	Wear Coeff
Ball	3200	3.10E+11	0.260	1.00E+10	2.00E−06
Races	7750	2.00E+11	0.250	7.84E+09	5.00E−06
Cage	1500	1.73E+09	0.300	1.00E+09	1.00E−05

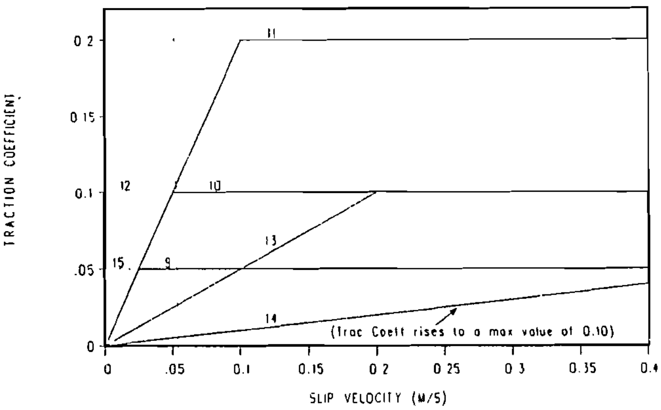

Fig. 4—Range of ball/race traction slopes and maximum traction coefficients.

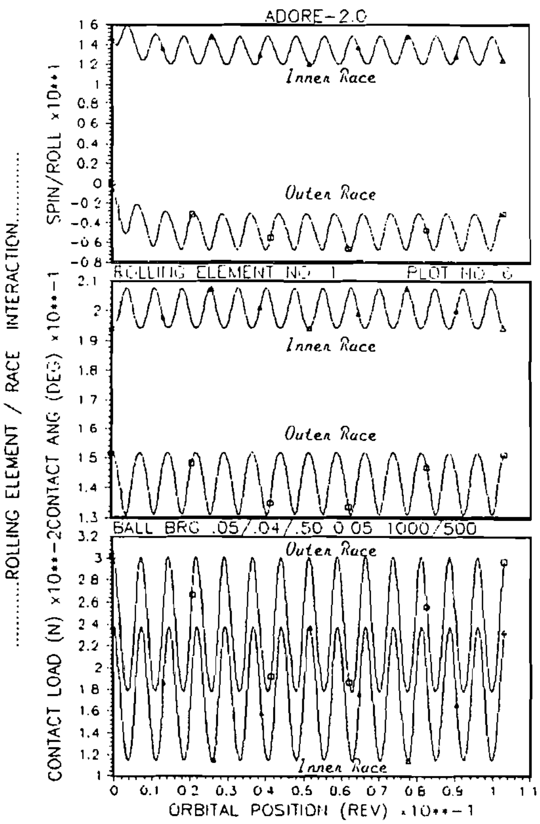

Fig. 5—Typical variations in ball/race contact load, angles and spin-to-roll ratios. Ball/race traction curve #1; cage friction coefficient = 0.050.

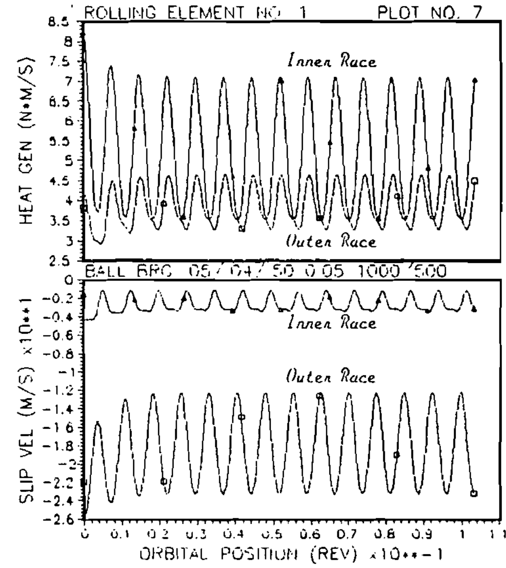

Fig. 6—Ball/race slip and heat generation in the contact. Ball/race traction curve #1; cage friction coefficient = 0.050.

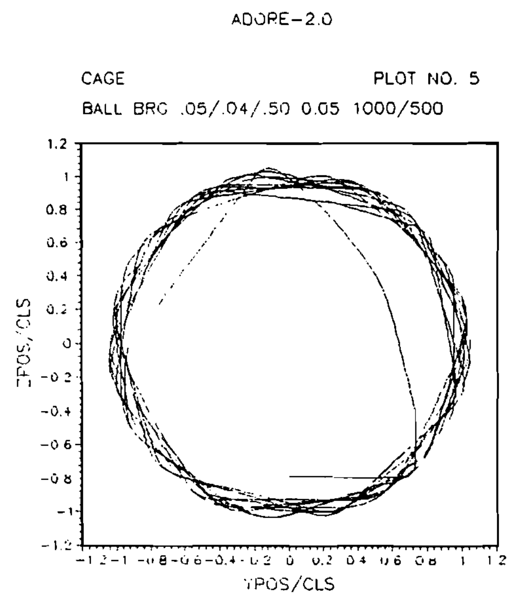

Fig. 7—Cage mass center whirl orbit with ball/race traction curve #1 and a cage friction coefficient of a 0.050.

around the bearing is due to rotation of the radial load with the shaft.

Also, note the spin-to-roll ratios plotted in Fig. 5; the ball spins on both races indicating that the conventional race control hypothesis (*23*) does not hold. The variations in ball slip, at center of the contact, and the overall heat generated in the ball/race contacts are shown in Fig. 6. The significantly higher heat generation at the inner race results from a higher spin velocity in the contact, as shown in Fig. 5. Thus, just the slip velocities at the center of the contact are not representative of the total energy dissipated at the ball/race interface.

Motion of the cage is fairly stable with the above frictional behavior. Figure 7 shows the simulated orbit of the cage mass center while the whirl and radial velocities are plotted in Fig. 8; the plotted whirl ratio denotes the ratio of mass center whirl to shaft angular velocity. The cage orbit varies from circular to somewhat polygonal; the circular part corresponds to lower radial velocities and a decreasing whirl ratio.

As the whirl velocity drops below the cage angular velocity, which is indicated by a ratio of about 0.42, the severity of cage/race contact increases which results in a step jump in whirl, change of orbit to a somewhat polygonal shape, and higher radial velocities of cage mass center. Such cyclic, saw-toothed, variations continue with an average whirl closely equal to the cage angular velocity.

The contact forces at the guide lands varies from about 2 to 4 N, see Fig. 9, while the pocket forces vary between 1 and 2 N. Figure 9 also shows the contact angle in a cage fixed-coordinate frame and the geometric interaction, which, when negative, essentially represents contact deflection; note

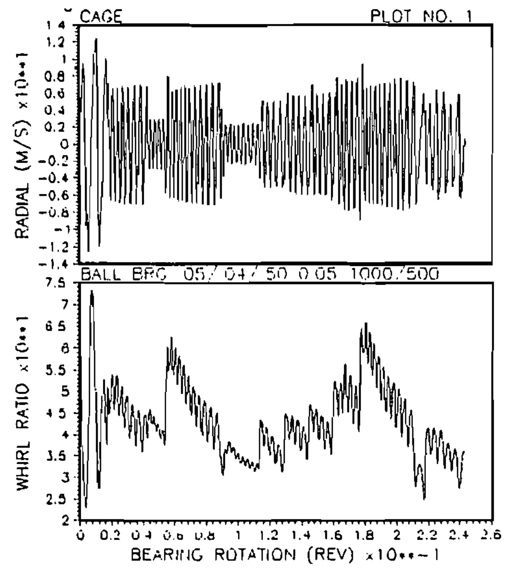

Fig. 8—Variation in cage mass center whirl and radial velocities with ball/race traction curve #1 and a cage friction coefficient of 0.050.

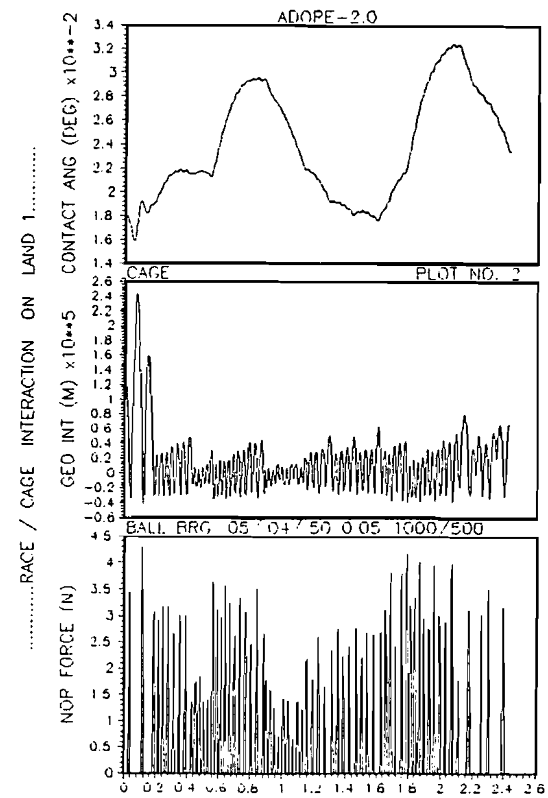

Fig. 9—Cage/race interaction under ball/race traction curve #1 and cage friction coefficient of 0.050.

that the trend in variation of geometric interaction corresponds directly to the variation in radial velocity of cage mass center shown in Fig. 8.

An interesting observation is the variation in cage/race contact angle; it is seen that over the twenty-five shaft revolutions simulated in Fig. 9, the contact angle varies between 180 and 320 degrees, which implies that less than half of the cage surface contacts the race and the resultant forces are somewhat fixed in the cage. Such an observation provides some support to the "biased cage designs" (*24*), where the cage is manufactured with a controlled unbalance, with the expectation that the rotating inertial force shall be in equilibrium with the ball/cage forces.

The overall level of the various interactions is shown in Fig. 10, where the time-averaged wear rates of the ball, races, and the cage are plotted. While the ball and race wear rates stabilize to a well-defined level, the cage wear rate seems to go through a cyclic variation with a trend of stabilization to a certain mean value. A close examination of Figs. 8 to 10 reveals that the positive gradients in the cage wear rate correspond to higher oscillations in radial velocity of the cage mass center, denoting a somewhat unstable situation, and the decreasing wear rates represent more favorable and stable operation. Such an observation confirms the stability hypothesis based on overall cage interactions, discussed above.

Once the overall stability of the bearing elements is ensured by steady values of the wear rates, solutions similar to the ones shown in Fig. 10 may be used for the estimation of wear life of a bearing. Thus, aside from establishing an overall stability, such simulations have a significant design potential.

As the ball/race traction level increases, the cage orbit becomes more polygonal and the whirl and radial velocities of the cage mass center exhibit increasing amplitude of variation; Fig. 11 shows the polygonal orbit obtained with traction curve #2 (see Fig. 3). The mass center velocities are similar to those shown in Fig. 8 with somewhat higher amplitudes.

Aside from the increasing level of instability with increasing traction, the negative slope of the ball/race traction relation also plays a dominant role in determining overall stability of the bearing elements. It is found that traction curve #3 exhibits an increased level of instability in comparison to curve #2. The impact of the negative traction slope is equally significant at lower values of traction also. For example, with traction curve #4, the cage motion stabilizes from an initially polygonal orbit to an almost circular stable orbit, as shown in Fig. 12, while traction relation #5 demonstrates excessive ball slip, increased pocket and guide land forces, and a more undesirable motion of the cage. When the negative traction slope is combined with higher maximum traction coefficients, for example traction curve #6, the ball slip velocities really become divergent, see Fig. 13.

Such progressively increasing slip velocities result in excessive interactions in the cage pockets; Fig. 14 shows the ball/cage force variation in three of the pockets. Note the excessive time of contact, which at the very high sliding velocities results in very rapid wear of the cage pockets and possibly a catastrophic cage failure; under more stable and favorable operation the ball/cage forces simply exhibit very narrow spikes, which imply extremely small contact times. Even with relatively higher traction levels, if the severity of the negative slope is reduced, the bearing operation becomes relatively stable. This is confirmed by bearing performance simulations obtained with traction curves #7 and #8. The steep traction slopes, typical of curve #6, are generally encountered with liquid lubricants at extremely high contact pressures (*25*), (*26*).

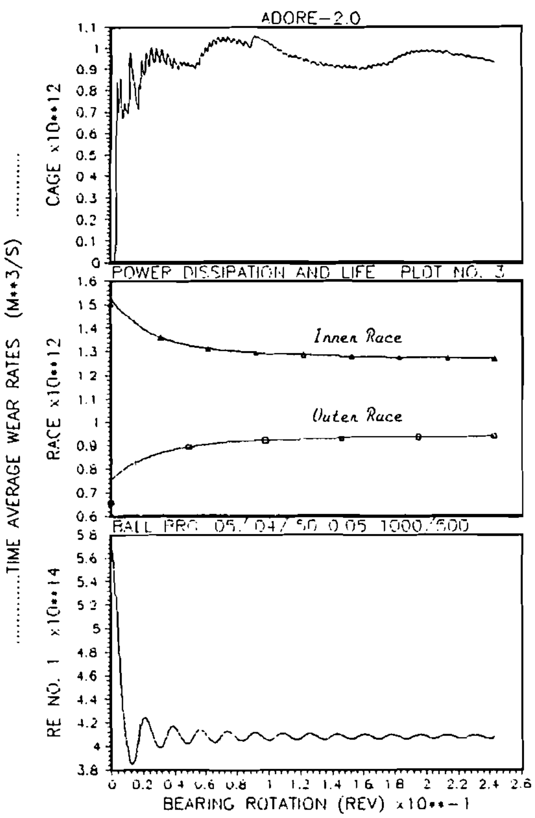

Fig. 10—Time-averaged wear rates of bearing elements under ball/race traction curve #1 and cage friction coefficient of 0.050

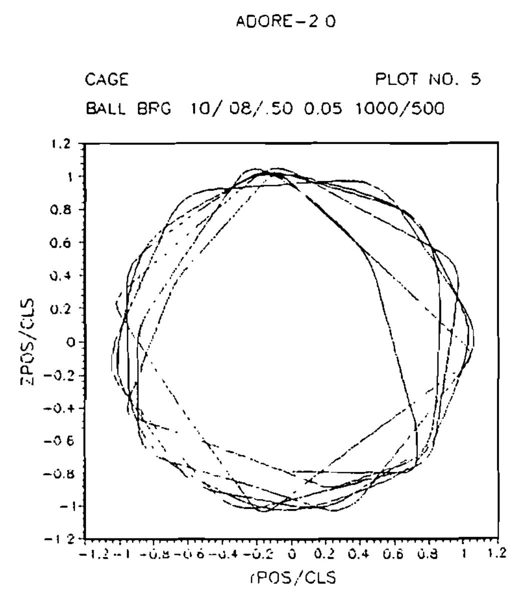

Fig. 11—Cage mass center orbit with ball/race traction curve #2 and cage friction coefficient of 0.050.

All of the results discussed thus far are obtained with a ball/cage and cage/race coefficient of friction of 0.050. In order to assess the sensitivity of cage motion to the level of cage friction, a number of simulations are obtained with varying cage friction, while the ball/race traction is held fixed. In fact, it is prescribed by somewhat simplified relations of Fig. 4, which are representative of solid lubricants (*15*), (*16*).

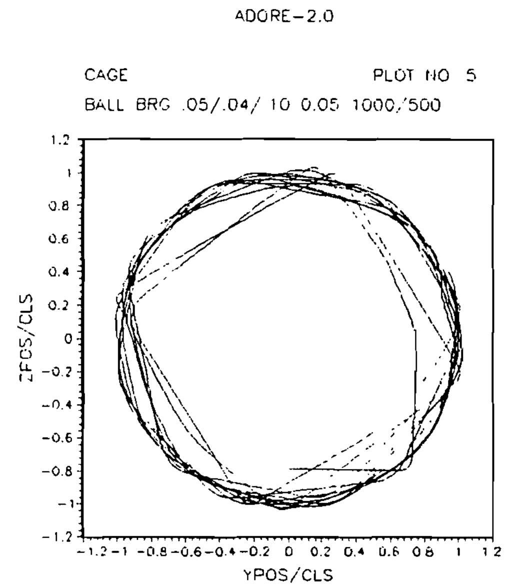

Fig. 12—Cage mass center orbit with ball/race traction curve #4 and cage friction coefficient of 0.050.

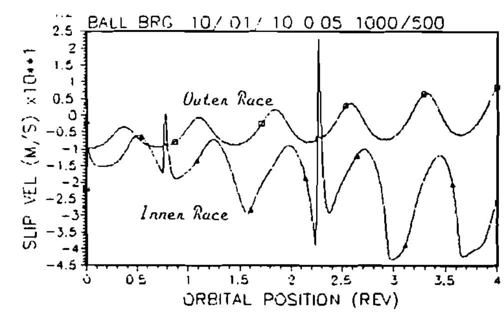

Fig. 13—Diverging ball/race slip with traction curve #6.

With the traction relation #9 (see Fig. 4), the cage friction coefficient is varied from 0.20 to 0.010. With a friction coefficient of 0.20, the cage starts out to be stable but the orbit rapidly becomes unstable. As shown in Fig. 15, the cage whirl orbit is almost circular at start, it gradually becomes polygonal and then completely unstable. The motion is more favorable with a friction coefficient of 0.10 but the stability is marginal. At a friction coefficient of 0.050, however, the motion is quite stable and the orbit is almost circular, as shown in Fig. 16. With a further decrease in cage friction, the motion becomes increasingly stable; the whirl orbit becomes quite circular, whirl velocity approaches the angular velocity of the cage, and, as shown in Fig. 17, the cage/race contact also becomes almost steady. Such a correlation of stability to cage friction is in complete agreement to that noted by Kannel and Bupara (*4*). The current results also seem to indicate that in the stable region of cage friction, the overall cage interaction and resulting cage wear is proportional to the cage friction coefficient. Such an observation has some design significance, although the present results are limited to establish a universal validity of such a trend.

Along with higher cage friction, as the ball/race traction is further increased, the cage orbits become highly unstable. Figure 18 shows the rather erratic, cage whirl orbit and the

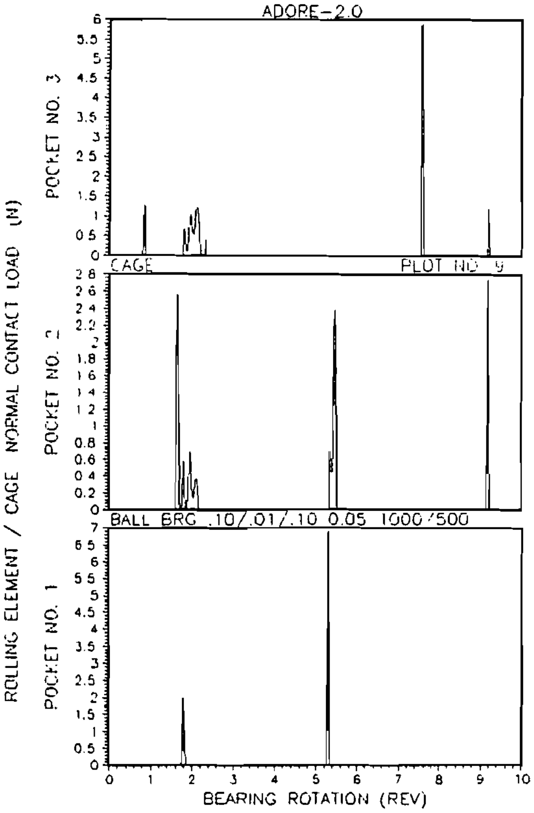

Fig. 14—Typical ball/cage contact forces with ball/race traction curve #6 and cage friction coefficient of 0.050.

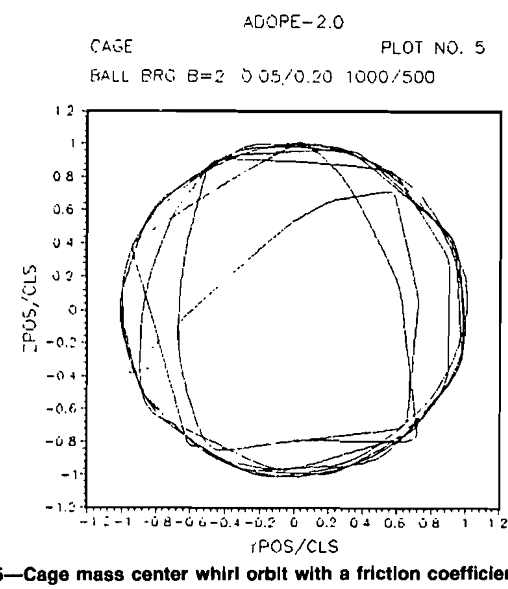

Fig. 15—Cage mass center whirl orbit with a friction coefficient of 0.20 and moderate level of ball/race traction.

corresponding cage/race collision forces, with traction relation #10 and cage friction coefficient of 0.20. Such a motion is not necessarily mechanically damaging to the cage, but large and rapid variations in whirl velocity indicate excessive squeal. As the cage friction is reduced to 0.050, the motion becomes more stable, the orbit remains highly polygonal, and the variations in whirl velocities continue to represent excessive squeal. Such observations are more pronounced when the ball/race traction is raised higher to curve #11 of Fig. 4.

Aside from a correlation of cage stability to friction, discussed above, Kannel and Bupara (*4*), (*13*) have postulated a rather simplified stability criterion in terms of the frictional energy dissipated at the ball/race contact and the ball/cage collision forces. In terms of this criterion, the cage may become unstable with an increasingly value of a damping number, defined as

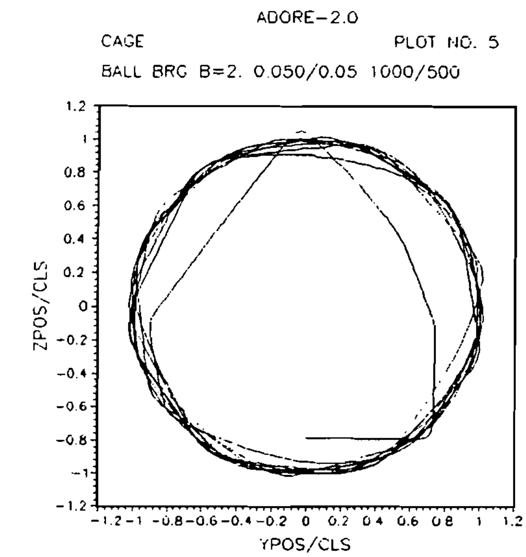

Fig. 16—Cage mass center whirl orbit with a friction coefficient of 0.050 and moderate level of ball/race traction.

$$D = \frac{8\bar{C}^2}{Mk}$$

where k is the ball/cage spring rate, M is the cage mass, and $\bar{C}$ is the ball/race "damping coefficient," defined in terms of ball/race traction, F and slip v,

$$F = \bar{C}v$$

In terms of the simplified traction curves discussed above, the ball/race damping coefficient, $\bar{C}$, for a prescribed ball/race contact load, is essentially equal to the traction slope in Fig. 4. Thus, in order to check the validity of the above criterion, a number of simulations are run with varying traction slopes. For a maximum traction coefficient of 0.10, the relations #12, #13, and #14, along with #10 provide a traction slope variation from infinity (constant friction coefficient) to a very low slope of 0.10 S/M. It is, indeed, found that the lower traction slope results in increased stability; cage motion is completely stable for curve #14, while it is grossly unstable at constant traction coefficient (relation #12); similar instabilities at constant traction coefficient have also been reported earlier by Gupta (*15*). However, at the lower value of maximum traction coefficient (0.05), the cage motion is found to be stable at all slopes of the traction curve, including a constant traction coefficient (relation #15 in Fig. 4). Similarly at higher levels of traction, 0.20 for example, the cage motion remains unstable at all values of traction slope, at least in terms of cage orbit shape, whirl velocity variation, and squeal.

The above results indicate that along with cage friction and ball/race traction slope, the level of ball/race traction at very high slip velocities has a controlling effect on cage

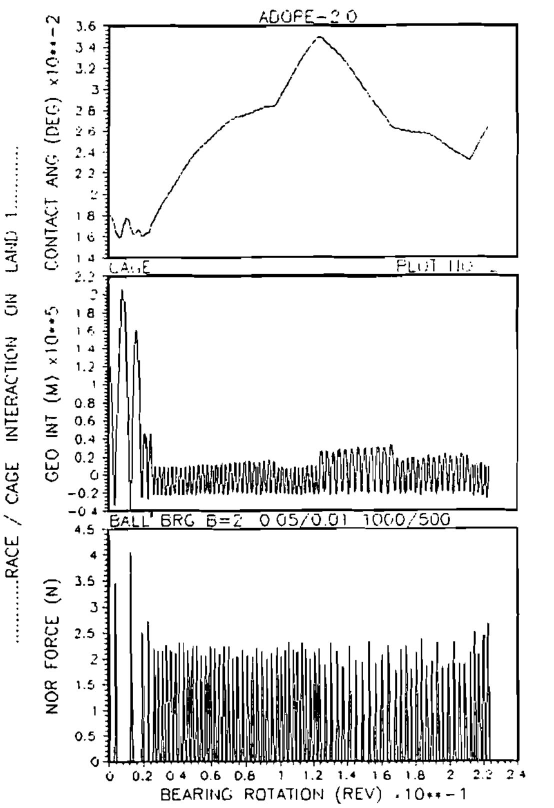

Fig. 17—Cage/race interaction under cage friction coefficient of 0.010 and moderate ball/race traction level.

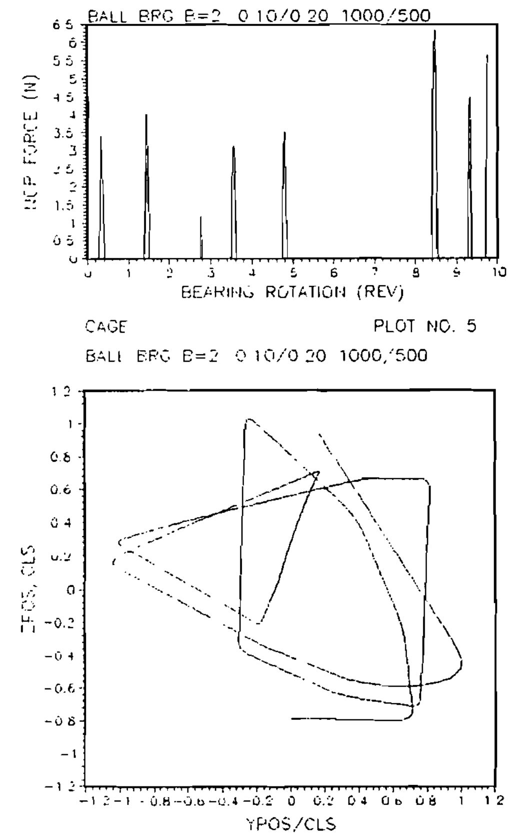

Fig. 18—Cage mass center whirl orbit and cage/race contact forces under relatively high ball/race traction (curve #10) and cage friction coefficient of 0.20.

stability. In fact, as shown above for traction curve #6 of Fig. 3, a steep negative traction slope at high-slip velocities, as found for liquid lubricants under very high contact pressures (*25*), (*26*), may result in the most damaging instabilities and catastrophic bearing failures. Although the development of a stability criterion which may be universally valid for all bearings under all operating conditions may be an extremely difficult task, the results of the present investigation do demonstrate a significant design potential for computer modeling and bearing performance simulation techniques in the development of acceptable designs.

CONCLUSIONS

Frictional instabilities of the cage and ball skid are correlated to the frictional behavior at the ball/race, ball/cage, and cage/race interactions in a high-speed ball bearing, and the feasibility of computer modeling approach to rolling bearing design is demonstrated. Although at overall low values of friction the bearing operation may be stable and relatively insensitive to the actual variation of traction or friction coefficients as a function of slip velocities, the traction/slip relations greatly dominate bearing stability as the traction levels become moderate. It is shown that both the traction slope at very low slip rates and the variation in traction at high-slip velocities control both ball skid and overall stability of cage motion.

With increasing level of ball/race traction and cage friction, the cage mass center orbits become highly polygonal to rather erratic and unstable. It is shown that over a certain range of friction behavior a correlation between cage stability and frictional behavior is possible. The ball/race traction slope at low slip velocities and the cage friction coefficient demonstrate direct correlation to shape of cage mass center whirl orbit, whirl velocity variation, and bearing squeal. The variation in ball/race traction at high slip velocity, in particular a negative traction slope, is shown to produce excessive ball skid and perhaps the most damaging instability of the cage, where the cage forces and sliding velocities progressively increase and lead to a physical destruction of the cage. In the stable mode of operation, the modeling approach provides meaningful time-averaged wear rates of the bearing elements which are directly useful in estimation of bearing wear life. The approach, therefore, has a significant design potential.

RECOMMENDATIONS

Results of the present investigation greatly establish the feasibility of computer modeling approach to rolling bearing design and performance diagnosis. The intricate coupling between frictional behavior at the various interactions between bearing elements and overall bearing performance suggests further investigations in a number of specific areas.

The research required to understand the influence of cage pocket and guide land clearances on the overall cage motion and stability is perhaps the next step in the development of guidance for bearing design. It is expected that for a prescribed frictional behavior the overall mechanical interactions of the cage shall strongly depend on the operating clearances. Thus, as the cage wears out, the increasing clearances may have a marked effect on stability and life of the bearing. Also, since interactions in the cage pocket are generally in the fore and aft directions, the geometrical interaction models in the present computer codes may eventually have to be extended to model elongated pockets. After establishing some correlation between the operating clearances and overall dynamic performance, a treatment of time-varying clearances, resulting from wear, shall be a rather ambitious step.

Since friction between interacting elements, bearing geometry, dynamic forces exerted on the cage, and the resulting wear are all very closely connected subjects, enhancements of the current interaction models for a more realistic simulation of adverse operating environment shall be greatly welcomed. In particular, since the highly dynamic forces exerted on the cage often result in high local stresses and possibly plastic deformation, the refinement of the current elastic model shall be a valuable contribution. Similarly, the computation of wear under prescribed loads and sliding velocities may be greatly advanced by incorporating the recently developed wear equations for advanced cage materials for solid-lubricated ball bearings.

Most of the simulations obtained in the present investigation seem to suggest that, at least under the selected operating conditions, the forces exerted on the cage at the guide lands are relatively fixed with respect to the cage. This implies that a carefully selected unbalance in the cage may result in some improvement in overall cage interactions and stability. In the past, such a speculation has been experimentally supported by the "biased cage designs." Thus, further investigations to establish the correlation between cage unbalance and stability may be very enlightening.

Bearing response to varying operating conditions has yet to be understood; such an understanding is essential in the development of optimum designs for bearings subjected to a wide range of adverse operating environments. Perhaps a parametric evaluation of significant operating parameters may provide the required insight for determination of stability domains over prescribed load cycles.

The present investigation addresses ball bearings only. Since the current computer codes do provide models for cylindrical, tapered, and, to some extent, spherical roller bearings, similar effort for these types of bearings may be readily carried out.

ACKNOWLEDGMENTS

The research reported herein was sponsored by the National Science Foundation under Phase I of the Small Business Innovation Research Program, Grant Number ISI-8560824. Computer support was provided by Murray Hill Super Computer Center at the AT&T Laboratories, Murray Hill, New Jersey.

REFERENCES

(1) Walters, C. T., "The Dynamics of Ball Bearings," *J. Lubr. Tech., ASME Trans.*, **93**, pp 1–10 (1971).

(2) Gupta, P. K., "Transient Ball Motion and Skid in Ball Bearings," *J. Lubr. Tech., ASME Trans.*, **97**, pp 261–269 (1975).

(3) Gupta, P. K., "Dynamics of Rolling Element Bearings Part VI: DREB Computer Program Manual," Technical Report MTI-77TR55, Mechanical Technology Inc., Latham, New York (1977).

(4) Kannel, J. W. and Bupara, S. S., "A Simplified Model of Cage Motion in Angular Contact Bearings Operating in the EHD Region," *J. Lubr. Tech., ASME Trans.*, **100**, pp 395–403 (1978).

(5) Gupta, P. K., "DREB: A New Tool for Rolling Bearing Performance Simulation," ASME Paper #78-DE-15, presented at the 1978 Design Engineering Conference, Chicago, Ill. (1978).

(6) Gupta, P. K., "Dynamics of Rolling Element Bearings: Parts I to IV," *J. Lubr. Tech., ASME Trans.*, **101**, pp 293–326 (1979).

(7) Brown, P. F., Carrano, M. J., Dobek, L. J., McFadden, R. J., Miner, J. R., and Robinson, J. D., "Main Shaft High-Speed Cylindrical Roller Bearings for Gas Turbine Engines: Parts I to IV," Technical Report NAPC-PE-60C, Naval Air Propulsion Center, Trenton, New Jersey and Wright-Patterson Air Force Base, Ohio (1980).

(8) Gupta, P. K., "Interactive Graphic Simulation of Rolling Element Bearings, Phase I: Low-Frequency Phenomena and RAPIDREB Development," U.S. Air Force Report AFWAL-TR-81-4148, Wright-Patterson Air Force Base, Ohio (1981).

(9) Conry, T. F., "Transient Dynamic Analysis of High-Speed Lightly Loaded Cylindrical Roller Bearing, Parts I and II," NASA Technical Reports 3334 and 3335, NASA Lewis Research Center, Cleveland, Ohio (1981).

(10) Gupta, P. K., "Simulation of Low-Frequency Components in the Dynamic Response of a Ball Bearing," Advances in Computer Aided Design, *Proc. 1982 ASLE/ASME Lubr. Conf.*, Washington, DC (1982).

(11) Gupta, P. K., *Advanced Dynamics of Rolling Elements*, Springer-Verlag (1984).

(12) Meeks, C. R. and Karen, O. Ng, "The Dynamics of Ball Separators in Ball Bearings, Part I: Analysis," *ASLE Trans.*, **28**, 3, pp 277–287. Meeks, C. R., "The Dynamics of Ball Separators in Ball Bearings, Part II: Results of Optimization Study," *ASLE Trans.*, **28**, 3, pp 288–295 (1985).

(13) Kannel, J. W., Bupara, S. S., and Pentlicki, C. J., "Investigation of Cage and Bearing Instability in Despun Antenna Bearings Due to Changes in Lubricant Properties," U.S. Air Force Report AFML-TR-75-38, Wright-Patterson Air Force Base, Ohio (1976).

(14) Kannel, J. W. and Snediker, D. K., "The Hidden Cause of Bearing Failure," *Machine Design*, April 7, pp 78–83 (1977).

(15) Gupta, P. K., "Some Dynamic Effects in a Solid-Lubricated Ball Bearing," *ASLE Trans.*, **26**, 3, pp 393–400 (1983).

(16) Bandow, H. E., Gray, S. E., and Gupta, P. K., "Performance Simulation of a Solid Lubricated Ball Bearing," ASLE Preprint No. 85-AM-4E-3.

(17) Kingsbury, E. P., "Torque Variations in Instrument Ball Bearings," M.I.T. Instrumentation Laboratory Report #E-1675, June 1964.

(18) Gupta, P. K. and Forster, N. H., "Modeling of Wear in a Solid-Lubricated Ball Bearing," *ASLE Trans.*, **30**, 1, pp 55–62 (1987).

(19) Gardos, M. N. and McConnell, B. D., "Development of a High-Load High-Temperature Self-Lubricating Composite, Parts I to IV", ASLE SP-9 (1982).

(20) Gardos, M. N., "Solid Lubricated Rolling Element Bearings Semiannual Status Reports No. 1 to 7," prepared for DARPA under Air Force Contract Number F33615-78-C-5196.

(21) Mecklenberg, K. R., "Lubricant Compact Wear Rate Techniques," Air Force Materials Laboratory Report, AFWAL-TR-81-4014, Wright-Patterson Air Force Base, Ohio, 1981.

(22) Meeks, C. R. and Bohner, J. J., "Predicting Life of Solid-Lubricated Ball Bearings", *ASLE Trans.*, **29**, 2, pp 203–213 (1986).

(23) Jones, A. B., "A General Theory for Elastically Constrained Ball and Radial Roller Bearings under Arbitrary Load and Speed Conditions," *J. Basic Eng., ASME Trans.*, **82D**, pp 309–320 (1960).

(24) Jacobsen, P. E., "Long Life Ball Bearing Suspension System, A Present Possibility," presented at AIAA Guidance and Control Conf., San Diego, California, 16–18 August, 1976.

(25) Gupta, P. K., Flamand, L., Berthe, D., and Godet, M., "On the Traction Behavior of Several Lubricants," *J. Lubr. Tech., ASME Trans.*, **103**, pp 55–64 (1981).

(26) Gupta, P. K., "Traction Modeling of Military Oils—Phase I," PKG Inc. Report G-104-86-TR, prepared for Wright-Patterson Air Force Base, Ohio, Contract No. F33615-85-C-2581, (1986).

DISCUSSION

T. F. CONRY
University of Illinois
Urbana, IL 61801

The simulation of the dynamic behavior of rolling element bearings is a difficult task indeed. Each ball interacts with the inner and outer race and, potentially, with the cage. The cage motion is dependent on the forces exerted by each ball on the cage and the interaction between the cage and guide land of the outer race. If the coefficient of friction in cage/ball contacts is low, the radial forces acting on the cage will consequently be low; if the coefficient of friction is high the radial forces will be high. The cage in a high speed bearing can be considered as an inertial ring with an angular momentum. The radial forces (there may also be an out-of-plane component) exerted on the cage will tend to move the center of mass of the ring away from the geometric center of the bearing, resulting in a higher drag torque exerted by the guide land clearance. High radial forces will tend to cause larger variations in radial motion and perturbations in the angular momentum of the ring. If these quantities are sufficiently large, cage instability can be expected.

The conclusions drawn in this paper are dependent on the traction model of the lubricant and on the numerical error in the integration scheme of the program. It has been shown (e.g. Conry, (*3*) and Conry, Johnson and Owen (*1*)) that as the temperature increases, the traction curves for lubricants migrate from those with negative slopes after having reached a peak to those that exhibit an almost constant traction at higher slip velocities. When lubricants are subjected to high slip at lower temperatures, the generated heat soon raises the temperature of the contacting surfaces. Given enough time a thermal equilibrium will be reached. When a bearing is started up, the surfaces are at a lower temperature then the eventual steady state operating temperature, and lubricant traction curves with negative slopes may be descriptive in this regime. The first question is, then, how does the thermal time constant of the bearing contact surface compare with the period of one revolution of the bearing?

The question is still open on the explanation of the negative slope in traction curves, though most evidence points to thermal effects as the cause of the negative slope, i.e. heat is generated faster than it can be transferred which results in a local temperature rise and a lower viscosity. The problem becomes more complex, however, when the contact is subjected to both slip and spin. Recent work by Conry (*4*) shows general agreement with the work of Daniels (*2*) on the temperature differences between the midplane and the race surfaces. A significant result obtained in this work, however, is the potentially very high surface temperatures over part of a contact with slip and spin. The highest temperatures occur in the regions with the highest shear rates, which only covers about half the area of contact. Clearly the prediction of average traction curves for slip and spin would be more difficult than for cases with no spin. Would the author please comment on the validity of using the traction curves in Figs. 3 and 4 for conditions where spin is present?

Lastly, in bearing dynamics, the impact of balls with the cage creates a more complex system, in fact, the system may be classified as stiff (the ratio of the largest to smallest eigenvalues is greater than 10). This has implications for the prediction of stability because numerical error is sometimes interpreted as a prediction of physical instability. How is the numerical error controlled in your program when the balls are impacting the cage?

REFERENCES

(*1*) Conry, T. F., Johnson, K. L., and Owen, S., "Viscosity in the Thermal Regime of EHD Traction," *Thermal Effects in Tribology*, D. Dowson, C. M. Taylor, M. Godet, D. Berthe, Editors, Mech. Eng. Pub. Ltd., London, pp 219–227.

(*2*) Daniels, B. K., "Non-Newtonian Thermo-Viscoelastic EHD Traction from Combined Slip and Spin," *STLE Trans.*, **23**, 2, pp 141–154 (1980).

(*3*) Conry, T. F., "Thermal Effects on Traction in EHD Lubrication," *J. of Lub. Tech.*, **103**, pp 533–538 (1981).

(*4*) Conry, T. F., "Thermal Effects on Traction in Elastohydrodynamic Lubrication," Final Rept., NSF MEA 82-05464, UILU-ENG-86-3026 p 71 (1986).

AUTHOR'S CLOSURE

The author fully agrees with Professor Conry that a real-time simulation of the dynamic performance of a ball bearing is a very difficult task. Both mechanical and thermal interactions play a dominant role in determining the overall bearing performance. The present work only models the mechanical interactions with a prescribed temperature field. Thus the specified tractions and the temperatures are closely equal to those expected at steady-state conditions. With such prescribed conditions the dynamic behavior of the bearing is solved strictly as a function of mechanical interactions between the various bearing elements. Typical time required for reaching steady-state is equivalent to about five to ten shaft revolutions depending on the tractions coefficients at the ball/race contacts, the frictional interactions at the cage interfaces and the overall mechanical interaction between bearing elements.

Traction behavior of lubricants in concentrated contacts in rolling bearings is again a very difficult subject. Primary objectives of the present investigation are to simply establish a correlation between friction behavior and instabilities in the motion of bearing elements. Thus all traction curves used are selected fairly arbitrarily. The question about validity of a specific traction curve under the operating conditions in a bearing is still open. However, the present results do provide some guidance for lubricant materials development by correlating bearing dynamics to traction behavior.

All numerical solutions in the present investigation are obtained by using a fifth order Runge-Kutta-Fehlberg explicit algorithm (*1*) for integrating a system of differential equations of motion. The local truncation error is, therefore, well controlled and stability is fully assured. Realistic modeling of the ball/cage collisions is accomplished by automating the step size with a prescribed limit on local truncation error. Thus when the ball collides with the cage, the step size is automatically reduced to closely simulate the collision with a greatly different time scale. Validity of the overall numerical approach has been tested by obtaining identical solutions with varying step sizes and order of the algorithms. In addition the overall cage motion, as predicted by the computer codes has been validated against actual experimental data (*2*). The results presented are, therefore, free of any numerical uncertainties and the correlations of cage instabilities to frictional behavior are significant.

REFERENCES

(*1*) Fehlberg, E., "Classical Fifth-, Sixth-, Seventh- and Eight-Order Runge-Kutta Formulas with Step Size Control," NASA Technical Report NASA TR R-287, George C. Marshall Space Flight Center, Alabama, (October 1968).

(*2*) Gupta, P. K., Dill, J. F., Artuso, J. W., and Forster, N. H., "Ball Bearing Response to Cage Unbalance," *ASME J. of Trib.*, **108**, 3, pp 462–467 (1986).